Robust Nonadaptive Three-Phase Quasi-Type-I PLL Approach under Distorted Grid Voltage Conditions

Anant Kumar Verma*, Claudio Burgos-Mellado†, Samir Gautam‡, Hafiz Ahmed§, Taesic Kim ¶,
Mohd. Afroz Akhtar‖, Giuseppe Fedele**, and Pedro Roncero-Sánchez††
*‡Institute of Engineering Sciences, Universidad de O'Higgins, Rancagua, Chile, 611
†School of EIE, University of Sydney, Australia, NSW 2006
§Nuclear Futures Institute, Bangor University, United Kingdom, LL57 1UT
¶Department of EECS, Texas A&M University, Kingsville, USA, 78363-8202
‖Aerosystems Laboratory, CSIR - CMERI, India, 713209
**DIMES, University of Calabria, Italy, 87036
††Department of EECEC, Universidad de Castilla-La Mancha, Spain, 13071
Email: *Anant.kumar@uoh.cl, †Claudio.burgos@uoh.cl, ‡Samir.gautam@sydney.edu.au, §Hafiz.h.ahmed@ieee.org,
¶Taesic.kim@tamuk.edu, ‖Afrozakhtar@cmeri.res.in, **Giuseppe.fedele@unical.it, ††Pedro.roncero@uclm.es

***Abstract*—In this article, a three-phase non-adaptive pre-filtered quasi-type-I (QTI) phase-locked loop (PLL) approach is proposed for fast detection of fundamental positive sequence components. For this purpose, a non-adaptive pre-filtering architecture that relies on Lyapunov estimation theory is investigated. It is noted that the Lyapunov's principle-based QTI-PLLs are sensitive to the presence of fundamental negative sequence (FNS), harmonics, and DC-offset components. Thus, it requires additional efforts to resolve the aforementioned issues. Since the internal state-variable feed-backs in the Lyapunov's demodulation approach leads to poor dynamic performance, an improved immunity against DC-offset, harmonics and the FNS are achieved by avoiding state-feedback paths. Consequently, the demodulated error signals in the dq-frame can further reduce the number of state variables and efficiently reject the FNS components. Finally, the numerical results demonstrate the efficacy of the proposed method with respect to an enhanced QTI-PLL approach.**

***Index Terms*—Demodulation, Lyapunov's filter, moving average filter (MAF), phase-locked loop (PLL), Three-phase systems**

I. Introduction

Synchronization constitutes an integral component in the control system of grid connected power converter in different applications namely photovoltaic (PV) systems, wind turbine (WT) systems, electric vehicle (EV) charging systems, active power filters, and uninterruptible power supply (UPS) [1]. Although various types of synchronization algorithm have been reported in literature, phase-locked loop (PLL) remains by far the most popular and preferred approach [2], [3]. Structurally, PLL is composed of three major functional units, i.e., a phase estimator (PE), a voltage controlled oscillator and a loop-filter [4]. The characteristics of a PLL is governed based on how a PE and a loop filter are implemented. In addition, the revision of grid codes and updated grid interconnection requirement of distributed generation have renewed the demand for efficient PLL techniques [5] [6]. The main aim is fast and accurate extraction of grid parameters despite the presence of grid disturbances, namely the fundamental negative sequence (FNS), harmonics, and the DC-offset, in the measured three-phase grid voltage signal [7]. The most appealing synchronous reference frame (SRF) PLL technique applicable to both three-phase and single-phase applications but has poor disturbance rejection ability which is dependent on the loop filter bandwidth [8]. Therefore filters are appended either before the PLL control loop, inside the control loop or in a hybrid manner to achieve operational robustness against disturbances [9]. A wide range of filtering solution were proposed such as moving average filter (MAF) [10], complex coefficient filter (CCF) [11], all-pass filter (APF) [12], delayed signal cancellation [13], notch filter [14] and second order generalized integrator (SOGI) [15]. The application of Lyapunov's theory based pre-filter in grid synchronization is also gaining momentum [16], [17].

Note that, if the filtering schemes are not efficiently designed, the improved robustness may come at the cost of longer transient and reduced stability margin. To address this issue, a quasi-type-I PLL (QTI-PLL) was proposed in [18] with faster estimation speed, higher disturbance rejection capability, while maintaining fair stability margin. The QTI-PLL inherits the structural simplicity of type-I PLL while exhibiting control aspects of type-2 which is necessary to eliminate phase error during grid frequency drifts. Several variants of the QT1-PLL are reported in literature with major distinction being on how filters are designed and implemented for different operating scenarios. In [19], a prefilter DSC is used for DC offset rejection and APF for orthogonal signal generation in QT1-PLL for single phase application. Similarly in [9], a frequency fixed modified DSC with arbitrary delay is used for DC offset rejection. A CCF based QT1-PLL is proposed in [7]. All aforementioned QT1-PLLs use frequency fixed filters wherein additional compensator network are included for error correction in estimated quantities under off-nominal frequency. A frequency adaptive MAF filter for QT1-PLL is implemented in [20] albeit with higher computational burden. Finally, the proposed work intends to mitigate the drawbacks associated with the recent Lyapunov's theory based QTI-PLL [19], [9] and is elaborated in the subsequent sections.

II. Problem Formulation

As per the recent grid code requirements [5], the (PV) systems should deliver required amount of reactive power

to the grid by supplying the reactive current within 30 ms during faulty conditions. Hence, the PV systems shall remain connected to the grid in order to provide dynamic support in the event of fault occurrence. The stable operating behavior of either a single or a three-phase grid-tied converter during the event of fault is ensured by quickly estimating the fundamental amplitude information [6]. As indicated by (1), the challenge with the single-phase estimation of grid voltage parameters is the availability of lesser information,

$$s(t) = A_1 \ \sin(\omega t + \Phi) \tag{1}$$

where, Φ, A_1, ω, and t are the initial phase angle, the fundamental amplitude, the angular grid frequency, and the instantaneous time period, respectively. The number of unknown parameters to be estimated in (1) are three i.e. amplitude, phase, and frequency. To address this challenge, an error demodulation approach based on Lyapunov's theory [21], [22] may be utilized which is responsible for the generation of the fundamental in-phase and quadrature components. This approach demonstrates more stable behavior in case of three-phase systems owing to the availability of the orthogonal components [17]. To some extent, the error demodulation approach is similar to the grid voltage demodulation, as the fixed-frequency and/or adaptive-frequency unit orthogonal components are utilized to extract the fundamental orthogonal signals. It is known that the conventional Lyapunov's estimator dealt in [21] is highly sensitive to DC-offset component. Thus, an extra DC-offset estimation loop can help reject the contamination of the DC-offset component contained in the grid voltage signal [16]. However, the slower dynamic response is the key property associated with the DC-offset estimation loop which might affects the overall dynamic performance of a synchronization scheme. To elevate this problem further, pre-rejection of DC-offset is carried out in [9] with additional computational load. Hence, the proposed approach can help address the aforementioned issues without additional efforts as follows:

- By eliminating internal state variable feed-backs.
- Fast pre-rejection of DC-offset component
- Utilizing error signals to estimate the fundamental positive sequence (FPS) components
- Taking advantage of QTI-PLL $dq-$frame filtering

A. Lyapunov's Estimation Law

In this section, a non-linear control theory based adpative Laypunov's filter (ALF) is discussed which was employed prior to the QTI-PLL approach acting as a pre-filter [9]. For the sake of simplicity, a single-phase grid voltage signal along with a DC-offset (s_{DC}) component is considered as follows:

$$s(t) = A_1 \ \sin(\omega t + \Phi) + s_{DC} \tag{2}$$

where Φ, A_1, and ω are the initial phase angle, the fundamental amplitude, and the angular grid frequency, respectively. Applying trigonometric identity, $s(t)$ is re-written as,

$$\begin{aligned} s(t) &= A_1 \ \cos(\Phi) \ \sin(\omega t) + A_1 \ \sin(\Phi) \ \cos(\omega t) + s_{DC} \\ &= s_1 \ S_o + s_2 \ C_o + s_{DC} \end{aligned} \tag{3}$$

where, $dq-$frame components (i.e., direct ($s_2 = A_1 \sin(\Phi)$) axis and quadrature ($s_1 = A_1 \cos(\Phi)$) axis), $S_o = \sin(\omega t)$, and $C_o = \cos(\omega t)$. Assuming grid frequency estimate ($\hat{\omega}$) is available through QTI-PLL (Fig. 1) then $S_o \rightarrow S_o = \sin(\hat{\omega} t)$ and $C_o \rightarrow C_o = \cos(\hat{\omega} t)$. Then, the estimate of $s(t)$ is,

$$\hat{s}(t) = \hat{s}_1 \ S_o + \hat{s}_2 \ C_o + \hat{s}_{DC} \tag{4}$$

where, the estimate of s_1, s_2, and s_{DC} are $\hat{s}_1$, $\hat{s}_2$, and $\hat{s}_{DC}$, respectively. The error between $s(t)$ and $\hat{s}(t)$ is,

$$\hat{e} = s - \hat{s} \tag{5}$$

$$= s_1 \ S_o + s_2 \ C_o + s_{DC} - \hat{s}_1 \ S_o - \hat{s}_2 \ C_o - \hat{s}_{DC} \tag{6}$$

As per the Lyapunov's estimation law [16], [17], the demodulation of $\hat{e}$ yields the estimated state variables as,

$$\dot{\hat{s}}_1(t) = k_e \ S_o \ \hat{e} \tag{7}$$

$$\dot{\hat{s}}_2(t) = k_e \ C_o \ \hat{e} \tag{8}$$

$$\dot{\hat{s}}_{DC}(t) = \gamma \ \hat{e} \tag{9}$$

where, k_e and γ are the tuning gain parameters for estimated $dq-$frame components and DC-offset component, respectively. Hence, it can be easily understood that the three state-variable must be estimated for proper operation of the ALF. Note that $k_e > \gamma$ consequently leads to a poor dynamic response and two tuning gain parameters are required to adequately tune the ALF. To address this challenge, a fast DC-offset rejecter unit is proposed as shown in Fig. 1 for pre-rejection of the DC-offset component present in the grid voltage signal. Despite

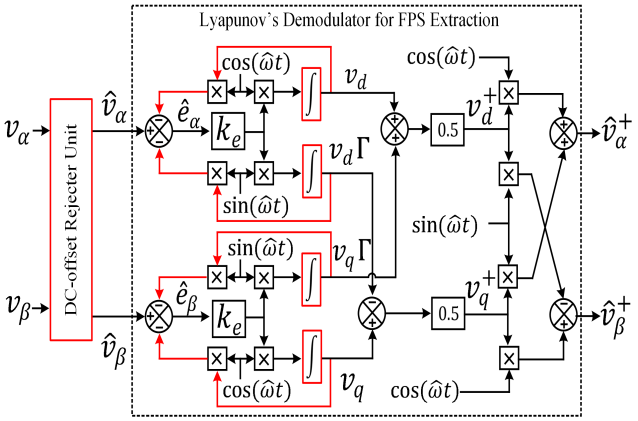

Fig. 1. Adaptive Lyapunov's-based FPS detection approach with DC-offset elimination capability.

the benefits, the proposal in [9] increases the computational complexity of the ALF structure and the dynamic response is still constraint to more than two fundamental cycles. Hence, the current proposal emphasizes on these critical issues by improvising the Lyapunov's approach in the subsequent section.

B. Proposed Non-adaptive Lyapunov's FPS detector

This section deals with the analysis focusing towards the proposed modified non-adaptive LF (MNLF) (Fig. 2) while considering the impact of DC-offset and harmonics. The stability concerns are already dealt in [17] and are avoided for

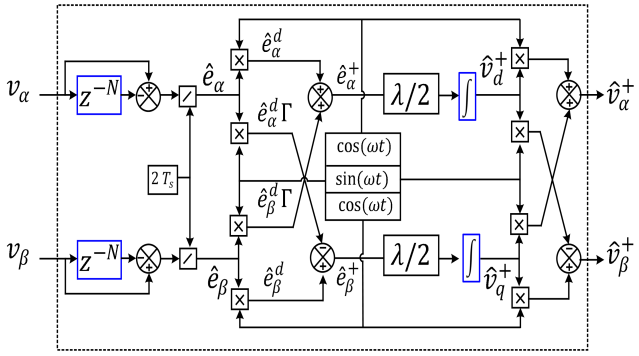

Fig. 2. Proposed MNLF based FPS detection approach.

the sake of brevity. To understand the modifications clearly, the single phase grid voltage signal may be considered as a reference. Later, the same is extended for three-phase power system applications.

C. Enhanced DC-Offset elimination capability

A discrete time grid voltage signal containing the DC-offset is examined as follows:

$$s(n) = A_1 \sin(\omega n T_s + \Phi) + V_o \tag{10}$$

where, T_s and n are the sampling time and the current sampling instant, respectively. The time-delayed version of $s(n)$ by N samples is denoted by,

$$s(n-N) = A_1 \sin(\omega n T_s + \Phi - N\omega T_s) + V_o \tag{11}$$

A comb filter structure introduced at the input side can help reject the DC-offset component and can rapidly estimate the error signal without the requirement of internal state variable feed-backs (compare Fig. 2 with Fig. 1 as regards the feedback paths highlighted in red) as follows:

$$\hat{e} = \frac{s(n) - s(n-N)}{2T_s} \tag{12}$$

It is intuitive that, $\hat{e}$ may be demodulated as per the Lyapunov's law of estimation to obtain $\dot{\hat{v}}_q$ and $\dot{\hat{v}}_d$ in their discrete form are given below:

$$\hat{v}_q(n) - \hat{v}_q(n-1) = \frac{\lambda\, S_n\, \hat{e}}{2} \tag{13}$$

$$\hat{v}_d(n) - \hat{v}_d(n-1) = \frac{\lambda\, C_n\, \hat{e}}{2} \tag{14}$$

where, $\lambda = 8 * f_n$ ([17]) is a fixed tuning gain parameter whereas $S_n = \sin(\omega t)$ and $C_n = \cos(\omega t)$ are tuned to $\omega_n = 2\pi f_n$ rad./s where $f_n = 50$ Hz. Thus, the third state variable for the estimation of DC-offset component is no more required. Also, the requirement of DC-offset rejection unit can be easily avoided. The parameter λ is obtained from the simplified transfer function relationships as follows:

$$\hat{V}_q(s) = \frac{\lambda}{2\,s}\hat{E}(s) \tag{15}$$

$$\hat{V}_d(s) = \frac{\lambda}{2\,s}\hat{E}(s) \tag{16}$$

For three-phase application, the grid voltage signal is decoupled into the $\alpha\beta-$axes components ($v_{\alpha\beta}$) using Clarke's transformation. Accordingly, the Lyapunov's estimation law is equally applicable to the error signals, i.e., $\hat{e}_\alpha$ and $\hat{e}_\beta$. Note that these errors can help extract the fundamental positive sequence components ($\hat{v}^+_{\alpha\beta}$) in a simplified way which help to reduce the number of integrators by two (see Fig. 2) as compared to the ALF (see Fig. 1).

D. FPS components extraction

In case of ALF, the orthogonal signals obtained from the Clarke's transformation are applied to two individual blocks of ALF, as shown in Fig. 1. Thereby, a pair of $dq-$frame components are easily obtained from v_α and v_β axes i.e. $\hat{v}_q$, $\hat{v}_q\Gamma$, $\hat{v}_d$, and $\hat{v}_d\Gamma$, where Γ represents the 90° shift. Using the instantaneous symmetrical component (ISC) method [17] [9], the FPS components ($\hat{v}_q^+$ & $\hat{v}_d^+$) from the pair of $dq-$frame components are easily obtained. In this numerical approach, four state-variables needs to be estimated, thus require four integrators to solve the FPS estimation problem. Hence, it is clear that the numerical approach adopted in [9] will lead to an unnecessary exploitation of hardware resources. To address this challenge, the ISC method is applied to the demodulated error ($\hat{e}_\alpha^d$, $\hat{e}_\alpha^q\Gamma$, $\hat{e}_\beta^q$, and $\hat{e}_\beta^d\Gamma$) signals of the proposed MNLF, which allows to estimate the $\hat{v}_q^+$ and $\hat{v}_d^+$ with reduced number of integrators as follows:

$$\begin{bmatrix}\hat{e}_\alpha^+\\ \hat{e}_\beta^+\end{bmatrix} = \frac{1}{2}\begin{bmatrix}1 & 1\end{bmatrix}\begin{bmatrix}\hat{e}_\alpha^d & -\hat{e}_\alpha^q\Gamma\\ \hat{e}_\beta^d\Gamma & \hat{e}_\beta^q\end{bmatrix} \tag{17}$$

Using (17), λ, and the Lypunov's estimation law, the FPS components are estimated as follows:

$$\dot{\hat{v}}_d^+(t) = \frac{\lambda}{2}\,\hat{e}_\alpha^+ = \frac{\lambda}{2}\,[\hat{e}_\alpha^d + \hat{e}_\beta^d\Gamma] \tag{18}$$

$$\dot{\hat{v}}_q^+(t) = \frac{\lambda}{2}\,\hat{e}_\beta^+ = \frac{\lambda}{2}\,[\hat{e}_\alpha^q - \hat{e}_\alpha^q\Gamma] \tag{19}$$

From (18) and (19), it is easily understood that the proposed MNLF offers to reduce the count of integrators and internal state-variables by a factor of two. Thus, allowing to attain a good simplicity as compared to [9]. Finally, the fundamental orthogonal components ($\hat{v}^+_{\alpha\beta}$) are obtained using an inverse Park's transformation. In view of the adoption of QTI-PLL approach, the proposed MNLF-based QTI-PLL can take advantage of a half-cycle MAF to attain better harmonic attenuation.

E. Enhanced Harmonic rejection capability

To observe the improvements achieved in the harmonic rejection ability the MNLF structure, a moving average filter (MAF) is deployed similar to [9], as shown in Fig. 3. Further, the benefits which MAFs bring to the MNLF structure are easily understood by considering a single-phase grid voltage signal consisting of a fundamental and a third harmonic component as follows:

$$s(n) = A_1 \sin(\omega\, n\, T_s + \Phi) + A_3 \sin(3\,\omega\, n\, T_s + \Phi_3) \tag{20}$$

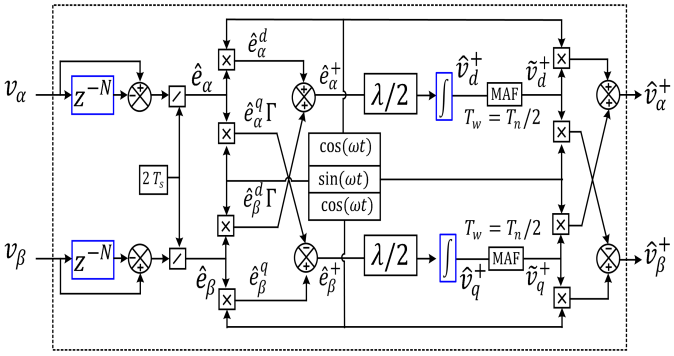

Fig. 3. Proposed MNLF involving half-cycle MAF.

where, A_3 and Φ_3 are the amplitude and the phase of 3^{rd} harmonic component, respectively. Similarly, the delayed version of $s(n)$ by N samples is,

$$s(n-N) = A_1\, sin(\omega n T_s + \Phi - N\omega T_s) + A_3\, sin(3\,\omega\, n\, T_s + \Phi_3 - 3NT_s) \quad (21)$$

Assuming $\omega = \omega_n$, $T_n = 2\pi/\omega_n$, and $N(=T/T_s$ where, $T = T_n)$. Then, the $\hat{e} \approx 0$ in the output of comb filter after N samples. However, $\hat{e} \neq 0$ under off-nominal frequency conditions. From (20), lets re-examine the state variables as:

$$\hat{v}_q(n) - \hat{v}_q(n-1) = \frac{\lambda\, S_n\, [s(n) - s(n-N)]}{4T_s} \quad (22)$$

$$\hat{v}_d(n) - \hat{v}_d(n-1) = \frac{\lambda\, C_n\, [s(n) - s(n-N)]}{4T_s} \quad (23)$$

From [17], it may be concluded that there exists second and even harmonic components in the expansion of (22) and (23). Thus, a MAF with a window length (T_w) equivalent to one-half of the fundamental period i.e. $T_w = T_n/2$, where $T_n = 1/f_n$ and $f_n = 50$ Hz can further enhance the second and even harmonic rejection abilities of MNLF. Later, the filtered $\tilde{v}_d^+$ and $\tilde{v}_q^+$ components are fed to an inverse Park's transformation to obtain the $\hat{v}_{\alpha\beta}^+$ components. In Fig. 4, magnitude response plots of ALF, MNLF with/ without MAF, ALF with DC-offset rejection unit (DRU) and ALF-DRU with MAF are compared. It is evident that the proposed MNLF-with MAF

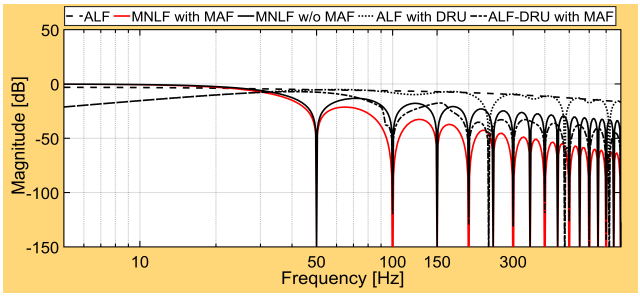

Fig. 4. Magnitude response plots of ALF, MNLF-OSG and MNLF with MAF.

structure offers better even harmonics components attenuation as compared to ALF, ALF-DRU, ALF-DRU with MAF and MNLF-without MAF. The step responses for MNLF-OSG and

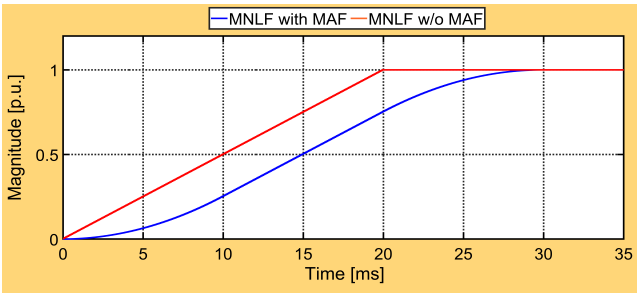

Fig. 5. Step response of MNLF-OSG and MNLF-OSG with MAF.

MNLF-MAF-OSG are provided in Fig. 5. At 50 Hz with $f_s = 1/T_s = 12$ kHz, the overall response time of the proposed MNLF-MAF-OSG is,

$$T_{net} = T_{COMB} + T_w \approx 1.5 * T_n = 30 \text{ ms} \quad (24)$$

It is to be noticed that, the response time of MNLF-OSG alone is 20 ms and with the inclusion of MAF with the $T_w = T_n/2$ is 30 ms.

III. Numerical Evaluation

In this section, the operation of the proposed QT1-PLL is evaluated in MATLAB/Simulink environment by emulating different test scenarios. Also, the QTI-PLL design is well-known in the literature and is avoided for the sake of brevity. Note that due to better pre-filtering capabilities of the proposed MNLF filter, the improvement in the bandwidth of QTI-PLL is possible. Thus, allowing to obtain improved dynamic response and the higher value selection of the control loop tuning parameter. Moreover to justify the competitiveness, the performance of the proposed QTI-PLL is compared with a recently reported enhanced QT1-PLL [9] which employs ALF-DRU with MAF and is hereafter referred to as EQT1-PLL. The control parameters for both the proposed and the EQT1-PLL [9] are given in Table I.

TABLE I
Design and Control Parameters of EQT1-PLL and Proposed PLL

Method	Parameters	Value
Simulation	Grid frequency	50 Hz
	Sampling frequency	12 kHz
EQT1-PLL	Proportional gain	61
	MAF window length	T/2
	Delay MDSC	50× 2
	Lyapunov filter gain	1600
Proposed PLL	MAF window length	T/2
	Proportional gain	1000
	Lyapunov filter gain (λ)	400

The following test cases are executed for evaluation purpose:

- Case I: $+30°$ of phase step: Fig. 6 illustrates the dynamic response of two PLLs in response to a abrupt phase transition of $+30°$. The proposed method not only yields

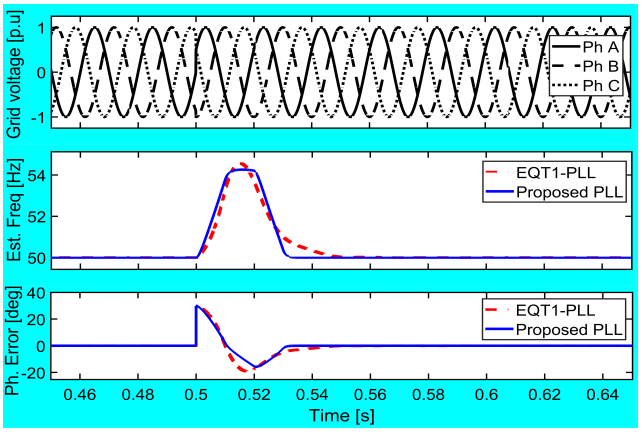

Fig. 6. Response of two PLLs for $+30^{\circ}$ jump as per Case I

a faster settling time but also exhibits a lower phase and frequency error during the transient.

- Case II: Frequency jump of $+2$ Hz: The dynamics associated with the frequency and phase tracking abilities in this case are exemplified in Fig. 7. Note that the EQT1-PLL suffers from a higher overshoot in the estimate of phase information as compared to the proposed PLL. Note that a better dynamic response, i.e., 30 ms to estimate the fundamental frequency information is offered by the proposed PLL. The details of measured 2% settling time and error values are quantitatively discussed in Table II.

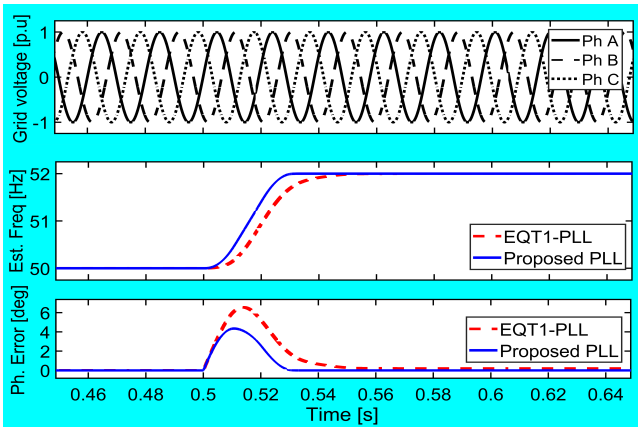

Fig. 7. Dynamic response in the event of +2 Hz step change in the grid frequency

TABLE II
DYNAMIC ASSESSMENT OF TWO QT1-PLLS

Test Case	EQT1-PLL [9]	Proposed QT1-PLL
+30° Phase Step		
2% settling time (ms)	46.03	31.18
Phase overshoot (%)	63.83	52.4
Peak Freq. error (Hz)	4.56	4.26
Frequency Jump (+2Hz)		
2 % settling time (ms)	45.74	28.27
Frequency overshoot (%)	0	0
Peak phase error (deg)	6.55	4.34

- Case III: Presence of DC offset and harmonics: The simulation result corresponding to this case is depicted in Fig. 8. The amount of DC offset and harmonics present

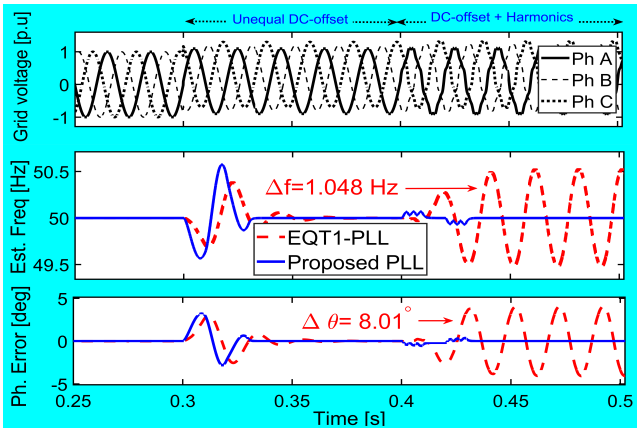

Fig. 8. Estimated phase and frequency from two PLLs as per Case III

in the grid voltage is shown in Fig. 8. At $t = 0.3$ s unbalanced DC offset are introduced into the measured three-phase grid voltage while harmonics are introduced at $t = 0.4$ s. Both the PLLs reject the impact of DC offset but the proposed method is able to do it swiftly within 30 ms. Moreover unlike the proposed method, the EQT1-PLL is incapable to completely attenuate the harmonic components which causes oscillation in the estimated quantities.

- Case IV: Presence of fundamental negative sequence component: In the final test case, the performance of both the PLLs are gauged for their ability to extract the fundamental positive/negative sequences. The associated simulation results are presented in Fig. 9.

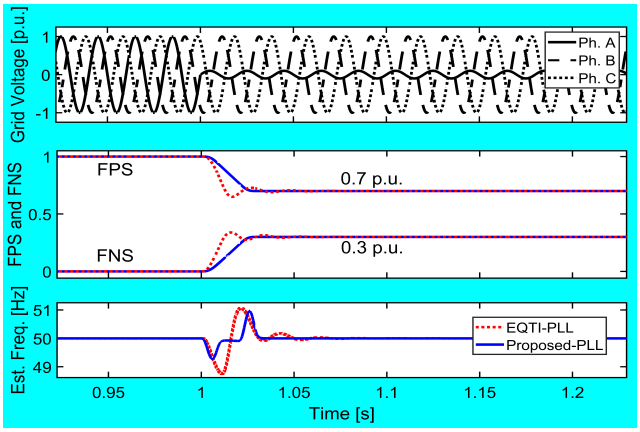

Fig. 9. Estimating the FNS and the FPS signals

Note that the proposed QTI-PLL is able to rapidly track the FPS and FNS sequence components as compared to the EQT1-PLL. Also, the overshoots in the estimate of fundamental frequency are lower in magnitude as compared the EQT1-PLL. Thus, it can be inferred that the proposed method exhibits an

improved transient response time and grid voltage disturbance rejection capabilities without applying additional efforts.

IV. Conclusion

This paper proposes an effective non-linear filtering technique based on Lyapunov's theory for rapid and easy determination of the FPS components. With the inclusion of a comb filter and a MAF in the MNLF-OSG structure, a good immunity is achieved against DC-offset and grid voltage harmonics. Simultaneously, the error demodulation approach can help to eliminate the requirements of additional state-variable feed-back loops. Thus, simplifying the design consideration as compared to the already known numerically complex approaches. Hence, a fast detection of grid voltage attributes (i.e. less than 40 ms) is possible with the proposed QTI-PLL. Moreover, the $dq-$frame based implementation of instantaneous symmetrical method allows to reject the FNS component within minimum number of MAFs. The results presented numerically demonstrated superiority of the proposed QTI-PLL with faster dynamic response and better steady state accuracy. The proposed QTI-PLL possess a good dynamic performance while rejecting the DC-offset, FNS, and the harmonics. With these potential improvements, the proposed MNLF-based QTI-PLL is useful for synchronization of three-phase power conditioning converters. The future plans are on extending and evaluating the current work's operation for a wider range of grid voltage disturbances and simplification in the design strategy.

References

[1] S. Gautam, W. Xiao, H. Ahmed, and D. D.-C. Lu, "Enhanced single-phase phase locked loop based on complex-coefficient filter," *IEEE Transactions on Instrumentation and Measurement*, vol. 71, pp. 1–8, 2022.

[2] R. Panigrahi, S. K. Mishra, S. C. Srivastava, A. K. Srivastava, and N. N. Schulz, "Grid integration of small-scale photovoltaic systems in secondary distribution network—a review," *IEEE Transactions on Industry Applications*, vol. 56, no. 3, pp. 3178–3195, 2020.

[3] S. Golestan, J. M. Guerrero, and J. C. Vasquez, "Single-phase plls: A review of recent advances," *IEEE Transactions on Power Electronics*, vol. 32, no. 12, pp. 9013–9030, 2017.

[4] P. Lamo, F. Lopez, A. Pigazo, and F. J. Azcondo, "An efficient fpga implementation of a quadrature signal-generation subsystem in srf plls in single-phase pfcs," *IEEE Transactions on Power Electronics*, vol. 32, no. 5, pp. 3959–3969, 2016.

[5] Z. Ali, N. Christofides, L. Hadjidemetriou, E. Kyriakides, Y. Yang, and F. Blaabjerg, "Three-phase phase-locked loop synchronization algorithms for grid-connected renewable energy systems: A review," *Renewable and Sustainable Energy Reviews*, vol. 90, pp. 434–452, 2018.

[6] Y. Yang, A. Sangwongwanich, H. Liu, and F. Blaabjerg, "Low voltage ride-through of two-stage grid-connected photovoltaic systems through the inherent linear power-voltage characteristic," in *2017 IEEE Applied Power Electronics Conference and Exposition (APEC)*, 2017, pp. 3582–3588.

[7] Y. Li, D. Wang, W. Han, S. Tan, and X. Guo, "Performance improvement of quasi-type-1 pll by using a complex notch filter," *IEEE Access*, vol. 4, pp. 6272–6282, 2016.

[8] S. Golestan, J. M. Guerrero, and J. C. Vasquez, "Three-phase plls: A review of recent advances," *IEEE Transactions on Power Electronics*, vol. 32, no. 3, pp. 1894–1907, 2016.

[9] H. Ahmed, Z. Tir, A. K. Verma, S. B. Elghali, and M. Benbouzid, "Quasi type-1 pll with tunable phase detector for unbalanced and distorted three-phase grid," *IEEE Transactions on Energy Conversion*, 2021.

[10] J. Li, Q. Wang, L. Xiao, Y. Hu, Q. Wu, and Z. Liu, "An $\alpha\beta$-frame moving average filter to improve the dynamic performance of phase-locked loop," *IEEE Access*, vol. 8, pp. 180 661–180 671, 2020.

[11] M. Ramezani, S. Golestan, S. Li, and J. M. Guerrero, "A simple approach to enhance the performance of complex-coefficient filter-based pll in grid-connected applications," *IEEE Transactions on Industrial Electronics*, vol. 65, no. 6, pp. 5081–5085, 2017.

[12] S. Golestan, J. M. Guerrero, J. C. Vasquez, A. M. Abusorrah, and Y. Al-Turki, "All-pass-filter-based pll systems: Linear modeling, analysis, and comparative evaluation," *IEEE Transactions on Power Electronics*, vol. 35, no. 4, pp. 3558–3572, 2019.

[13] Q. Huang and K. Rajashekara, "An improved delayed signal cancellation pll for fast grid synchronization under distorted and unbalanced grid condition," *IEEE Transactions on Industry Applications*, vol. 53, no. 5, pp. 4985–4997, 2017.

[14] H. Khazraj, F. F. da Silva, C. L. Bak, and S. Golestan, "Analysis and design of notch filter-based plls for grid-connected applications," *Electric Power Systems Research*, vol. 147, pp. 62–69, 2017.

[15] J. Xu, H. Qian, Y. Hu, S. Bian, and S. Xie, "Overview of sogi-based single-phase phase-locked loops for grid synchronization under complex grid conditions," *IEEE Access*, vol. 9, pp. 39 275–39 291, 2021.

[16] H. Ahmed and M. Benbouzid, "Demodulation type single-phase pll with dc offset rejection," *Electronics Letters*, vol. 56, no. 7, pp. 344–347, 2020.

[17] A. K. Verma, C. Subramanian, R. K. Jarial, P. Roncero-Sánchez, and U. M. Rao, "A robust lyapunov's demodulator for tracking of single-/three-phase grid voltage variables," *IEEE Transactions on Instrumentation and Measurement*, vol. 70, pp. 1–11, 2020.

[18] S. Golestan, F. D. Freijedo, A. Vidal, J. M. Guerrero, and J. Doval-Gandoy, "A quasi-type-1 phase-locked loop structure," *IEEE Transactions on Power Electronics*, vol. 29, no. 12, pp. 6264–6270, 2014.

[19] H. Ahmed, S. Biricik, H. Komurcugil, and M. Benbouzid, "Enhanced quasi type-1 pll-based multi-functional control of single-phase dynamic voltage restorer," *Applied Sciences*, vol. 12, no. 1, p. 146, 2021.

[20] W. Luo and D. Wei, "A frequency-adaptive improved moving-average-filter-based quasi-type-1 pll for adverse grid conditions," *IEEE Access*, vol. 8, pp. 54 145–54 153, 2020.

[21] D. Abramovitch, "Lyapunov redesign of analog phase-lock loops," *IEEE Transactions on Communications*, vol. 38, no. 12, pp. 2197–2202, 1990.

[22] G. Pin, B. Chen, G. Fedele, and T. Parisini, "Robust frequency-adaptive quadrature phase-locked-loops with lyapunov-certified global stability," *IEEE Transactions on Control Systems Technology*, pp. 1–8, 2022.